KAPL-P-000121
(K98163)

PERFORMANCE STATUS OF 0.55 eV InGaAs THERMOPHOTOVOLTAIC CELLS

CONF-981055--

S. Wojtczuk, G. W. Charache, D. M. DePoy

October 1998

NOTICE

KAPL ATOMIC POWER LABORATORY SCHENECTADY, NEW YORK 12301

Operated for the U. S. Department of Energy
by KAPL, Inc. a Lockheed Martin company

DISCLAIMER

DISCLAIMER

Portions of this document may be illegible in electronic image products. Images are produced from the best available original document.

Performance Status of 0.55eV InGaAs Thermophotovoltaic Cells

S. Wojtczuk[a], P. Colter[a], G. Charache[b] and D. DePoy[b]

a) Spire Corporation, One Patriots Park, Bedford, MA 01730-2396
b) Lockheed-Martin Inc., Schenectady, NY 12301

Abstract: Data on ~0.55eV $In_{0.72}Ga_{0.28}As$ cells with an average open-circuit voltage (Voc) of 298mV (standard deviation 7mV) at an average short-circuit current density of 1.16 A/cm^2 (sdev. 0.1 A/cm^2) and an average fill-factor of 61.6% (sdev. 2.8%) is reported. The absorption coefficient of $In_{0.72}Ga_{0.28}As$ was measured by a differential transmission technique. We use a numerical integration of the absorption data to determine the radiative recombination coefficient for $In_{0.72}Ga_{0.28}As$. Using this absorption data and simple one-dimensional analytical formula the above cells are modelled. The models show that the cells may be limited more by Auger recombination rather than Shockley-Read-Hall (SRH) recombination at dislocation centers caused by the 1.3% lattice mismatch of the cell to the host InP wafer.

Introduction

Low bandgap photovoltaic cells are needed for thermophotovoltaic (TPV) systems which utilize an appreciable portion of the thermal photons emitted from the heat sources of 1200C or less (Table 1). In this paper, we give material and cell performance data on 0.55eV $In_{0.72}Ga_{0.28}As$ TPV cells, including measured absorption coefficient data.

Table 1 *% of Energy From Blackbody Falling Below Cutoff Wavelength*

Cell Bandgap	Cell Materials	Cell Cutoff	Blackbody Temperature 1000C	1100C	1200C
1.1eV	Si	1.1μm	*0.9%*	*1.5%*	*2.2%*
~0.7eV	Ge, GaSb, $In_{0.53}Ga_{0.47}As$	~1.8μm	*12%*	*16%*	*20%*
~0.55eV	$In_{0.72}Ga_{0.28}As$, InGaAsSb	~2.3μm	*26%*	*31%*	*36%*

Absorption Coefficient Data

In order to model quantum efficiency, absorption coefficient data are needed. We measured the transmission versus wavelength through two thicknesses of undoped 0.55eV $In_{0.72}Ga_{0.28}As$, 0.1 and 1μm thick. These epilayers were grown on semi-insulating InP wafers to lower free-carrier absorption (InP transparent at $\lambda > 930$nm). Double-side polished wafers were used to minimize surface scattering.

Transmission data was taken in 20 nm increments from 1200 to 2340nm using light from a grating monochromator at near-normal incidence on the polished InP side of the test sample. This air/InP interface reflects ~27% of the incident light (InP refractive index is ~3.15 over 1200-2400nm[1]). The slight non-normal incidence eliminates reflected light. The transmitted light transits through the 600μm InP wafer, impinging on the $In_{0.72}Ga_{0.28}As$ film. The reflection at this middle InP/$In_{0.72}Ga_{0.28}As$ interface is negligible (~0.4%) since the refractive index of $In_{0.72}Ga_{0.28}As$ (estimated as 3.6) is close to that of InP. A portion of the beam is absorbed as it transits across the InGaAs film. Finally, the light impinges upon the $In_{0.72}Ga_{0.28}As$/air interface, where ~68% of the light exits out of the epilayer and is collected into an integrating sphere.

We then consider multiple reflections in the measurement. About 32% of the light beam is reflected at the final $In_{0.72}Ga_{0.28}As$/air interface, makes a second pass through the InGaAs, passes through the InP, and eventually ~27% is reflected from the initial InP/air interface, which then makes a third pass through the InGaAs before again arriving at the $In_{0.72}Ga_{0.28}As$/air interface. This sequence is repeated infinitely. Ignoring the InP/InGaAs interface due to its small reflection (~0.4%), and calling the air/InP and InGaAs/air reflections equal (R~0.3), the transmission is[2]:

$$T = \frac{(1-R)^2 e^{-\alpha L}}{1-R^2 e^{-2\alpha L}}$$

To find the InGaAs absorption coefficient, α, at each wavelength, we ratio the measured transmission intensities T_1 and T_2 for thicknesses L1 and L2:

$$\log\frac{T_1}{T_2} = \log\frac{(1-R^2)e^{-\alpha L_1}}{(1-R^2)e^{-\alpha L_2}} + \log\frac{1-R^2e^{-2\alpha L_2}}{1-R^2e^{-2\alpha L_1}} \approx \alpha(L_2 - L_1) + O(0.1)$$

Then, $\exp(-2\alpha L)$ can at most vary between 0 and 1. Therefore, the natural log of the second fraction can at most be 0.105 (i.e., on the order of 0.1 or O(0.1)). Thus, the data in Figure 1 is calculated from:

$$\alpha = \frac{\log(T_1 / T_2)}{L_2 - L_1} \pm \frac{1}{2}\frac{O(0.1)}{L_2 - L_1} = \frac{\log(T_1 / T_2)}{L_2 - L_1} \pm 500 cm^{-1}$$

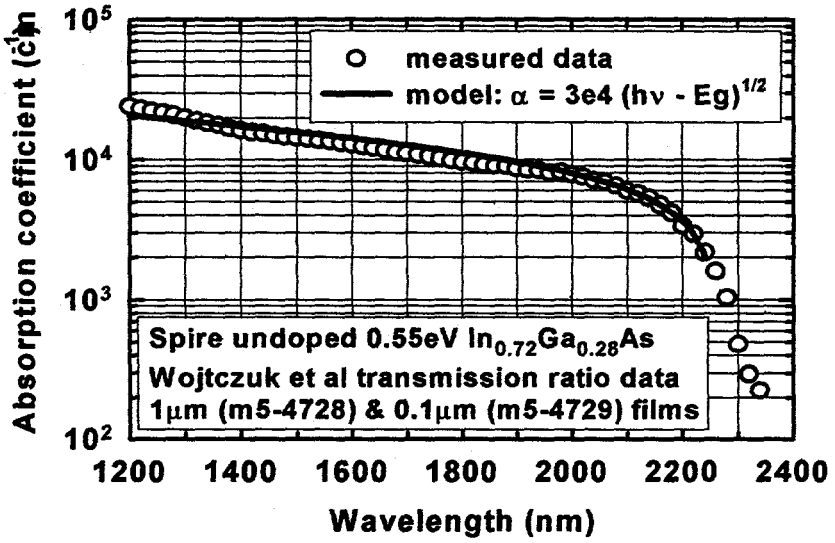

FIGURE 1. Measured 0.55eV $In_{0.72}Ga_{0.28}As$ absorption coefficient data and model fit.

Note that the above absorption data is accurate for a lightly-doped base region of a TPV cell, and for moderately doped P-type regions (before band-tailing due to impurity bands becomes noticeable). However, it is not at all accurate for a heavily-doped ($>10^{19}$ cm^{-3}) N-type emitter region for an N-on-P cell. Charache et al. have shown[3] that heavily-doped N-type InGaAs exhibits a pronounced Moss-Burstein shift (i.e., semiconductors with a small effective mass become optically transparent when the available states at the conduction band edge are filled with equilibrium electrons). Heavily-doped N-type InGaAs is significantly more transparent than would be ordinarily expected. The optical bandgap is ~1 eV for a nominally 0.6 eV electrical bandgap 10^{19} cm^{-3} N-type InGaAs.

Lifetime Model

The absorption coefficient data was numerically integrated to obtain the radiative lifetime recombination coefficient[4] B:

$$B = \frac{8\pi(kT)^3}{n_{iMM}{}^2 c^2 h^3} \sum_{\lambda} \frac{n_r^2 \alpha(\lambda) \left(\frac{hc}{\lambda kT}\right)^2}{\exp\left(\frac{hc}{\lambda kT}\right) - 1} \left(\frac{hcd\lambda}{\lambda^2 kT}\right) = 1.9x10^{-10} \frac{cm^3}{s}$$

where k, T, c, and h have their usual meaning, and the refractive index n_r of the material was assumed constant at 3.5 in this calculation, and the $d\lambda$ increment was 20nm with the range λ from 1200 to 2400nm. The intrinsic carrier concentration was obtained with effective masses that were linearly interpolated for the $In_{0.72}Ga_{0.28}As$ composition from the GaAs and InAs endpoints. The result was the effective electron mass was $0.036m_o$ and the hole mass was $0.417m_o$, leading to an intrinsic carrier concentration n_{iMM} of about $1.6x10^{16}$ cm^{-3} at 300K for $In_{0.72}Ga_{0.28}As$. Although we did not perform the integration to wavelengths shorter than 1200nm, almost all of the contribution to the integral is from the region around the bandgap edge; the omitted wavelengths contribute negligibly to the value of the sum.

For small-bandgap doped semiconductors, Auger recombination is a major limit to the lifetime. Since Auger recombination processes vary significantly and has not been measured directly, the Auger recombination coefficient will be estimated. We begin by noting for 0.74eV lattice-matched $In_{0.53}Ga_{0.47}As$ the intrinsic Auger recombination coefficient[5] C_{LM} is on the order of $8x10^{-29}$ cm^6/s. Then a similar coefficient C_{MM} for the lattice mismatched $In_{0.72}Ga_{0.28}As$ is calculated by scaling this value according to the simple theory[6]:

$$C_{MM} \approx C_{LM} \frac{\left(\frac{qEg_{LM}}{kT}\right)^{1.5} \exp\left(\frac{1+2M_{LM}}{1+M_{LM}} \frac{qEg_{LM}}{kT}\right)}{\left(\frac{qEg_{MM}}{kT}\right)^{1.5} \exp\left(\frac{1+2M_{MM}}{1+M_{MM}} \frac{qEg_{MM}}{kT}\right)} \frac{n_{iLM}^2}{n_{iMM}^2} = C_{LM} 5.2 = 10^{-27} \frac{cm^6}{s}$$

where Eg are the bandgaps, M_{MM} is the mass ratio for lattice mismatched

material (m_e/m_h or 0.036/0.417), M_{LM} is lattice-matched (0.044/0.436), and the lattice-matched intrinsic carrier concentration n_{iLM} is $8.7x10^{11}$ cm^{-3}. The overall lifetime is then calculated as

$$\tau(n) = \frac{1}{\frac{1}{\tau_{RADIATIVE}} + \frac{1}{\tau_{AUGER}} + \frac{1}{\tau_{SRH}}} = \frac{1}{Bn + Cn^2 + \frac{1}{\tau_{SRH}}}$$

where the above expression is assumed identical for electrons or holes. The non-radiative Shockley-Read-Hall lifetime, τ_{SRH}, was included for completeness. However, the open-circuit voltage of the model described later in this paper agrees with measured cells quite well without the SRH lifetime, which is due primarily to recombination at dislocations.. The open-circuit voltage is used for this purpose since it is the cell parameter that is most sensitive to dark current and therefore lifetime. **This is a surprising result. The cell is dominated by Auger recombination at high dopings, and radiative recombination at lower dopings. The SRH dislocation lifetime is negligible compared to these in the present 1.3% mismatch material.** This data can be used to bound the dislocation lifetime limit; and it is on the order of 100nS or more. Figure 2 shows the estimate of lifetime versus doping.

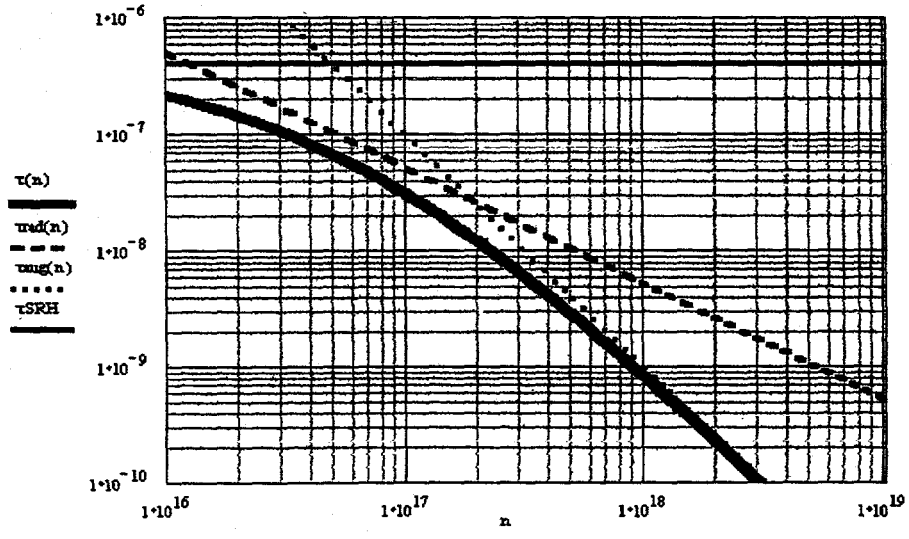

FIGURE 2. Calculated minority carrier (electron or hole) lifetime (s) vs. doping (cm^{-3}) for 0.55eV $In_{0.72}Ga_{0.28}As$. Thick solid line is overall lifetime; thin solid line is SRH dislocation lifetime bound; dotted line is Auger recombination, which is dominant at doping levels above $3x10^{17}$ cm^{-3}; and dashed line is the radiative recombination lifetime, which is dominant at lower dopings.

Mobility and Diffusion Length Models

The minority carrier diffusion lengths must be estimated to model a cell. We have measured *majority* carrier electron and hole mobility over a wide range of dopings[7] for 0.55eV InGaAs material. An empirical model fit to the referenced data is given as:

$$\mu e(n) = 1000 + \frac{10000}{1+\sqrt{\frac{n}{4x10^{17}}}} \qquad \mu h(p) = 60 + \frac{120}{1+\sqrt{\frac{p}{4x10^{17}}}} \frac{cm^2}{Vs}$$

We assume that minority carrier electrons in P-material have a mobility equal to electrons in N-material with the same doping level. This is equivalent to saying that the ionized impurity scattering is proportional to the total number of ionized impurities, but is independent of the sign of the impurity charges. Using the above mobility and lifetime models, the diffusion lengths were estimated as shown in Figure 3.

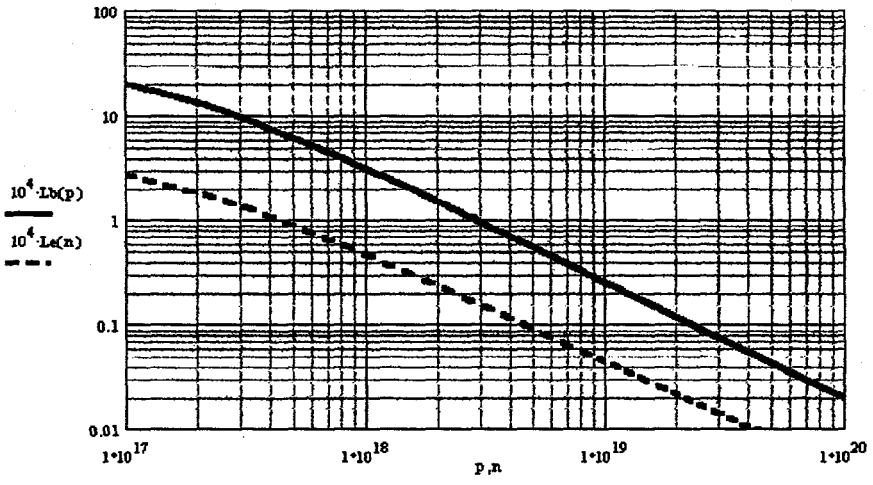

FIGURE 3. Calculated minority carrier base electron (solid line) and emitter hole (dotted) diffusion lengths (microns) vs. doping (cm^{-3}) for 0.55eV $In_{0.72}Ga_{0.28}As$.

Quantum Efficiency Models

With the absorption coefficient and diffusion length data given earlier, it is possible to model the N-on-P ~0.55eV cell described in Table 2.

Table 2 *Structure of N/P $In_{0.72}Ga_{0.28}As$ TPV Cell (Spire 6114-4646-10)*

Layer	Composition	Doping cm^{-3}	Thickness μm
Emitter	$In_{0.72}Ga_{0.28}As$	Se. $4x10^{19}$	0.1
Base	$In_{0.72}Ga_{0.28}As$	Zn, $3x10^{17}$	3.6
BSF	$InAs_{0.4}P_{0.6}$	Zn, $9x10^{17}$	0.05
Grade	$In_{0.72\ to\ 0.53}Ga_{0.28\ to\ 0.22}As$	Zn, $1x10^{19}$	4.0
Wafer	InP	Zn, $3x10^{18}$	600

Hovel[8] gives a complete model of photocurrent contributions from the emitter, base, and space-charge region. However, the heavily-doped emitter in our N-on-P cell is only 0.1μm, and because of the Moss-Burstein shift, this layer is transparent to wavelengths longer than 1200nm. Since shorter wavelengths are of limited interest for TPV cells, modeling the emitter is not profitable. Similarly, the above dopings demonstrate that the space-charge region is only 0.05μm. Negligible errors are made if we simply assume all of the light is absorbed in the base. Thus, we use Hovel's term:

$$\eta = \frac{R\alpha L}{\alpha^2 L^2 - 1}\left(\alpha L - \frac{\frac{SL}{D}\left(\cosh\left(\frac{t}{L}\right) - e^{-\alpha t}\right) + \sinh\left(\frac{t}{L}\right) + \alpha L e^{-\alpha t}}{\frac{SL}{D}\sinh\left(\frac{t}{L}\right) + \cosh\left(\frac{t}{L}\right)}\right)$$

where the term R accounts for the surface reflectivity (0.7), L is the base electron diffusion length at the doping given in Table 2 (see Fig.3, 10μm), D is the diffusivity at that same doping calculated from the given mobility model (~170 cm^2/s), S is the back surface interface recombination velocity between the $In_{0.72}Ga_{0.28}As$ and $InAs_{0.4}P_{0.6}$ taken as 10^4 cm/s, and t is the cell thickness (3.6μm - the sum of the emitter and base epilayers).

Figure 4 shows the fit between the above model and the actual measured data for the cell. The fit is fairly good; the only slight adjustment made to the model described above is that the bandgap was changed from 0.55eV to 0.57eV to match the model cutoff wavelength with the measured cell data. In practice, this is a shift of about 2% in In composition, which is consistent with our long-term run-to-run uniformity in the Metalorganic Chemical Vapor Depostion (MOCVD) epitaxial growth of these complex structures.

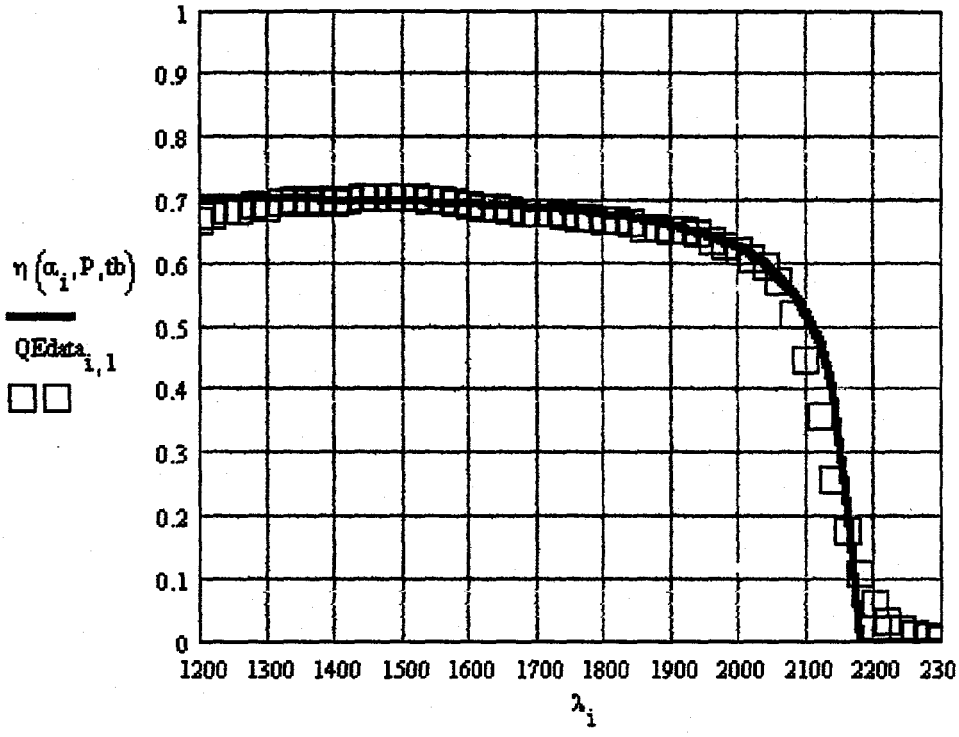

FIGURE 4. Comparison of measured QE data (squares) of cell of Table 2 with model of cell given by the above equation (solid line).

Dark Current Model

Although the calculation is not repeated here, the generation-recombination (n=2) dark current is only 1% of the diffusion dark current for these ~0.55eV cells at a bias of ~0.3V. Therefore, as expected, diffusion current dominates low-bandgap cells, and the space-charge-region generation-recombination term is ignored. The emitter hole diffusion length L_{EMIT} can be read from Figure 3 as 0.01μm for the structure of Table 2. The emitter is 10 times thicker, and therefore, a simple long-emitter diffusion model is appropriate. **Note that this implies that the cell dark current is quite insensitive to the front surface recombination velocity.**

The base electron diffusion length L_{BASE} is 10μm (same as in the QE model) from Figure 3 for the doping in Table 2. The base thickness is

only 3.5μm; therefore, we expect that a good low recombination back surface field (BSF) $InAs_XP_{1-X}$ layer can help the cell. The dark current[9] model is therefore:

$$JoB = \frac{qD_{BASE}n_i^2}{L_{BASE}P}\left(\frac{\frac{SL_{BASE}}{D_{BASE}}\cosh\left(\frac{t}{L_{BASE}}\right)+\sinh\left(\frac{t}{L_{BASE}}\right)}{\frac{SL_{BASE}}{D_{BASE}}\sinh\left(\frac{t}{L_{BASE}}\right)+\cosh\left(\frac{t}{L_{BASE}}\right)}\right)$$

$$JoB = \frac{qD_{BASE}n_i^2}{L_{BASE}P}0.385 = 8x10^{-6}\,A/cm^2 \quad JoE = \frac{qD_{EMIT}n_i^2}{L_{EMIT}N} = 1.7x10^{-6}\,A/cm^2$$

All of the terms have the same values and meaning as in the QE model section and n_i is the same value ($1.6x10^{16}$ cm^{-3}) as in the radiative lifetime model Dopings and thicknesses are given in Table 2. D_{EMIT} is 1.8 cm^2/s using the mobility formula given earlier. Note that the BSF lowers the diffusion current to only 39% of the value that would occur with a very thick base This corresponds to an increase of at least 25 mV to the cell open circuit voltage. The dark current contribution from the emitter is not negligible and is roughly 20% of the total diffusion current.

I-V Model

The I-V model is compared using the above dark currents and a cell series resistance[10] Rs (0.025 Ω-cm^2) and short-circuit current Jsc (1.1 A/cm^2) with an actual I-V (Figure 5) using the model:

$$J = (JoE + JoB)\left(\exp\left(\frac{q(V - JRs)}{kT}\right) - 1\right) - Jsc$$

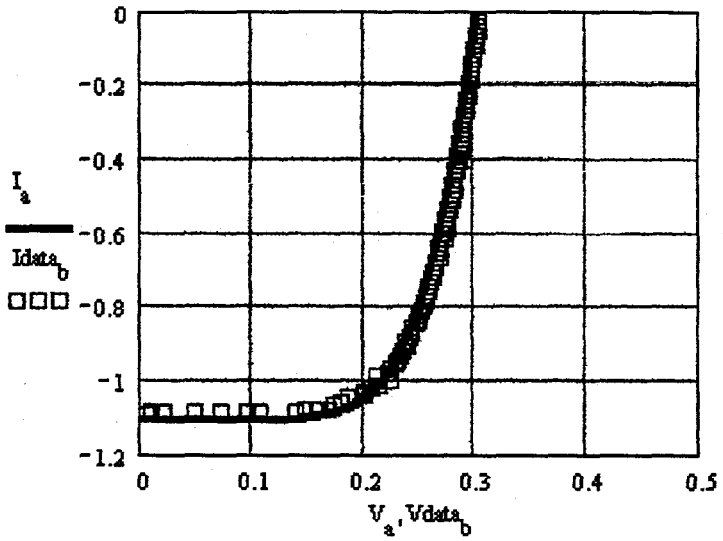

FIGURE 5. Measured IV data (squares) of cell of Table 2 with model (solid line).

Table 3 shows the data agreement. As a note, the series resistance Rs is limited mainly by the back alloyed AuZn contact to the InP wafer.

Table 3 *Comparison of Measured I-V data vs. Dark-Current I-V Model*

	Cell 6114-4646-10	Wafer Avg. 6114-4646	I-V Model
Voc	305mV	298mV	303mV
Jsc	1.12A/cm^2	1.17A/cm^2	1.12A/cm^2
Fill Factor	64%	62%	65%

Summary

We present a complete quantum efficiency and dark current model of an N/P $In_{0.72}Ga_{0.28}As$ cell. Fits between model and measured data are good. We describe a measurement and give absorption coefficient data for 0.55eV $In_{0.72}Ga_{0.28}As$, which is not widely available. Interesting results are: (1) lifetime in 1.3% lattice-mismatched $In_{0.72}Ga_{0.28}As$ seems limited by Auger recombination and not dislocation defects; (2) an N/P cell with a heavily doped emitter has a hole diffusion length of ~0.01μm and is insensitive to front surface recombination since emitters tend to be ~10X thicker to lower resistance for high currents; and (3) an effective back surface field adds at least kT/q ln (1/0.385) or 25mV to the cell Voc.

References

[1] Palik, E.D. , *Handbook of Optical Constants*, Academic Press, 1985, p. 512.

[2] Pankove, J.I. *Optical Processes in Semiconductors, Dover, 1975, p. 93.*

[3] Charache, G.W., DePoy, D.M., Egley, J.L., Dziendziel, R.J., Freeman, M.J., Baldasaro, P.F., Campbell, B.C., Sharps, P.R., Timmons, M.L., Fahey, R.E., Zhang, K., Borrego, J.M., "Electrical and Optical Properties of Degeneratively-Doped N-type $In_XGa_{1-X}As$", 3rd NREL TPV Conf., AIP Proc. 401, 1997, pp.215-226.

[4] Pankove, op. cit., pp. 108-111.

[5] Ahrenkiel, R.K., R. Ellington, S. Johnson, and Wanlass, M., "Recombination Lifetime of $In_{0.53}Ga_{0.47}As$ as a Function of Doping Density," Appl. Phys. Lett., **72**, 3470 (1998).

[6] Pankove, op. cit., p. 162.

[7] Wojtczuk, S. "Comparison of 0.55eV InGaAs Single-Junction vs. Multi-junction TPV Technology," 3rd NREL TPV Conf., AIP Proc. 401, 1997, pp.205-213.

[8] Hovel, *Solar Cells,* Semiconductors and Semimetals v.11, Academic, 1975, pp.17-20.

[9] Hovel, op. cit., p. 51.

[10] Wojtczuk, S. "$In_XGa_{1-X}As$ TPV Experiment-based Performance Models," 2nd NREL TPV Conf., AIP Proc. 358, 1995, pp. 387-393.